Annals of Nuclear Medicine Vol. 19, No. 4, 283–290, 2005

Apparent CBF decrease with normal aging due to partial volume effects: MR-based partial volume correction on CBF SPECT

Kentaro INOUE, Hiroshi ITO, Ryoi GOTO, Manabu NAKAGAWA, Shigeo KINOMURA, Tachio SATO, Kazunori SATO and Hiroshi FUKUDA

Department of Nuclear Medicine and Radiology, Institute of Development, Aging and Cancer, Tohoku University

Several studies using single photon emission tomography (SPECT) have shown changes in cerebral blood flow (CBF) with age, which were associated with partial volume effects by some authors. Some studies have also demonstrated gender-related differences in CBF. The present study aimed to examine age and gender effects on CBF SPECT images obtained using the ^{99m}Tc-ethyl cysteinate dimer and a SPECT scanner, before and after partial volume correction (PVC) using magnetic resonance (MR) imaging. Forty-four healthy subjects (29 males and 15 females; age range, 27–64 y; mean age, 50.0 ± 9.8 y) participated. Each MR image was segmented to yield grey and white matter images and coregistered to a corresponding SPECT image, followed by convolution to approximate the SPECT spatial resolution. PVC-SPECT images were produced using the convoluted grey matter MR (GM-MR) and white matter MR images. The age and gender effects were assessed using SPM99. Decreases with age were detected in the anterolateral prefrontal cortex and in areas along the lateral sulcus and the lateral ventricle, bilaterally, in the GM-MR images and the SPECT images. In the PVC-SPECT images, decreases in CBF in the lateral prefrontal cortex lost their statistical significance. Decreases in CBF with age found along the lateral sulcus and the lateral ventricle, on the other hand, remained statistically significant, but observation of the spatially normalized MR images suggests that these findings are associated with the dilatation of the lateral sulcus and lateral ventricle, which was not completely compensated for by the spatial normalization procedure. Our present study demonstrated that age effects on CBF in healthy subjects could reflect morphological differences with age in grey matter.

Key words: SPECT, partial volume effects, age, brain atrophy, MRI

INTRODUCTION

MANY STUDIES using positron emission tomography (PET) or single photon emission computed tomography (SPECT) have investigated whether cerebral blood flow (CBF) decreases with normal aging, because changes in CBF with normal aging would confound the interpretation of results of CBF imaging studies of neurodegenerative and neuropsy-chiatric disorders. CBF SPECT has been widely used in clinical settings, due to its relatively high availability compared with PET. Several studies using technetium 99m (^{99m}Tc)-labeled tracers have repeatedly revealed CBF changes with age.[1–9] Gender-related differences in CBF have also been investigated, indicating that females have higher global and regional CBFs than males,[10,11] and that there are gender-related differences in the regional CBF pattern.[4,12,13]

Due to a relatively poor spatial resolution, SPECT as well as PET images suffer from partial volume effect (PVE).[14] PVE can cause an apparent decrease in the uptake of PET or SPECT tracers in small or atrophic structures, and it can confound our understanding of aging or disease processes. Several authors, therefore, have reported the methods of partial volume correction for PET

Received January 19, 2005, revision accepted March 14, 2005.

For reprint contact: Kentaro Inoue, M.D., Department of Nuclear Medicine and Radiology, Institute of Development, Aging and Cancer, Tohoku University, 4–1 Seiryo-machi, Aoba-ku, Sendai 980–8575, JAPAN.

E-mail: kenta@idac.tohoku.ac.jp

using high resolution morphologic information obtained from magnetic resonance (MR) images.[15–19] Over the past few years, progress in processing software has facilitated automated voxel-by-voxel analysis for brain morphometry using magnetic resonance (MR) imaging data.[20,21] This progress has enhanced the investigation of regional morphological differences in the entire brain using MR images subjectively, and regional morphometric changes in the brain with age,[22,23] gender-related morphological differences,[24] as well as relationships between brain atrophy and age effects on CBF[25,26] have been demonstrated. Van Laere et al. (2001) compared CBF SPECT data with MR morphometric data, and showed that decreases in CBF and in grey matter (GM) concentration[20] with age were parallel, and also showed that there was no significant disagreement between CBF and GM concentration in gender-related differences.[25] In our previous study, we also observed that decreases in CBF with age were parallel with, and statistically less significant than, those in GM concentration.[26] It was also demonstrated that metabolic changes associated with disease processes that were obscured by brain atrophy could be clarified by PVC.[27–29] Few studies, however, have examined the effect of PVC on normal subjects. Meltzer et al. (2000) suggested that an apparent decrease in CBF with age measured using $H_2{}^{15}O$ PET results from the confounding effects of brain atrophy.[30] Matsuda et al. (2003), on the other hand, demonstrated in their study using male subjects and SPECT that, in several brain areas, CBF decrease with age remained statistically significant even after PVC.[31]

The aim of the present study was to investigate the effects of PVC on age and the effects of gender on CBF SPECT images. For this purpose, age and gender effects on CBF SPECT using the ^{99m}Tc-labeled ethylene cysteinate dimer (^{99m}Tc-ECD) were examined on SPECT images before and after PVC using MR images of the brain. We compared these results with those of MR morphometric analysis using voxel-based morphometry (VBM)[20] on age and gender effects in the same subjects.

MATERIAL AND METHODS

Subjects

Forty-four healthy volunteers (29 males; mean age, 48.9 ± 10.8 y; range, 27–63 y; 15 females; mean age, 52.0 ± 7.3 y; range, 37–64 y) participated in the study. They were participants in a research program on brain aging in city dwellers conducted by the Institute of Development, Aging and Cancer, Tohoku University. As described previously,[26] only those with normal T1- and T2-weighted MR images of the brain, or minor hyperintensities on a T2-weighted image in the deep white matter or periventricular white matter, were recruited for the present study. None of the participants had a history of a major medical, neurological, or psychiatric disease. The study was approved by the local ethics committee of the Institution of Development, Aging and Cancer, Tohoku University. Written informed consent was obtained from all the subjects after a proper explanation of the study was provided, according to the Code of Ethics of the World Medical Association (Declaration of Helsinki).

SPECT

Image acquisition was performed with a four-head gamma camera (SPECT-2000H; Hitachi Medico Corp., Tokyo, Japan) with an in-plane and axial resolution of 8-mm full-width at half-maximum (FWHM). The camera was fitted with a low-energy, high-resolution collimator. Each subject lay in the supine position with the eyes closed during both the injection of approximately 800 MBq ^{99m}Tc-ECD and the subsequent SPECT measurements obtained about 10 min after the ^{99m}Tc-ECD injection, as described before to be feasible.[32] Sixty-four projections at 20 s (20 s × four heads = total 80 s) per projection, with a 360° rotation of the camera, were acquired. Image reconstruction was performed by filtered backprojection using a Butterworth filter (dimension, 12; cut-off frequency, 0.25 cycles/pixel) resulting in a spatial resolution of 10.6 mm. Attenuation correction was performed numerically, assuming an elliptical object shape for each slice and a uniform attenuation coefficient (0.1 cm^{-1}) (Chang's method). No correction was performed for scattered photons. Image slices were arranged parallel to the orbitomeatal line and obtained at 8-mm intervals throughout the entire brain.

MR

All MR imaging studies were performed using a Signa 0.5-Tesla system (General Electric, Milwaukee, WI, USA). A three-dimensional volumetric acquisition of a

Fig. 3 Scatter plots of age versus CBF in male subjects, which normalized to the global mean of 50, in the right anterolateral PFC (a), left caudate head (b), and right cerebellum (c). Before PVC; filled circle and solid line, after PVC; open circle and dotted line. Note that a significant correlation was found before PVC in the anterolateral PFC and the caudate head, but not in the cerebellum. PVC changed the correlation in the anterolateral PFC, but had little effect on the caudate head and cerebellum.

Fig. 4 Spatially normalized MR images of demonstrable cases of a young male subject (*up*) and an old male subject (*bottom*) (a). Areas which showed statistically significant decrease in GM concentration with age (see Fig. 2) were superimposed on the mean of the spatially normalized GM mask images without smoothing (b). Note that the global size and shape of the brain were comparable between the young and old subjects, but the widening of the lateral sulcus and the lateral ventricle was not compensated for in the old subject. The area in the lateral PFC, which lost statistical significance in the age effects after PVC, is located within the mean GM mask image. On the other hand, the area around the lateral sulcus and ventricles, where statistically significant age effects were found before and after PVC, is located on the edge of the mean GM mask image.

Fig. 1

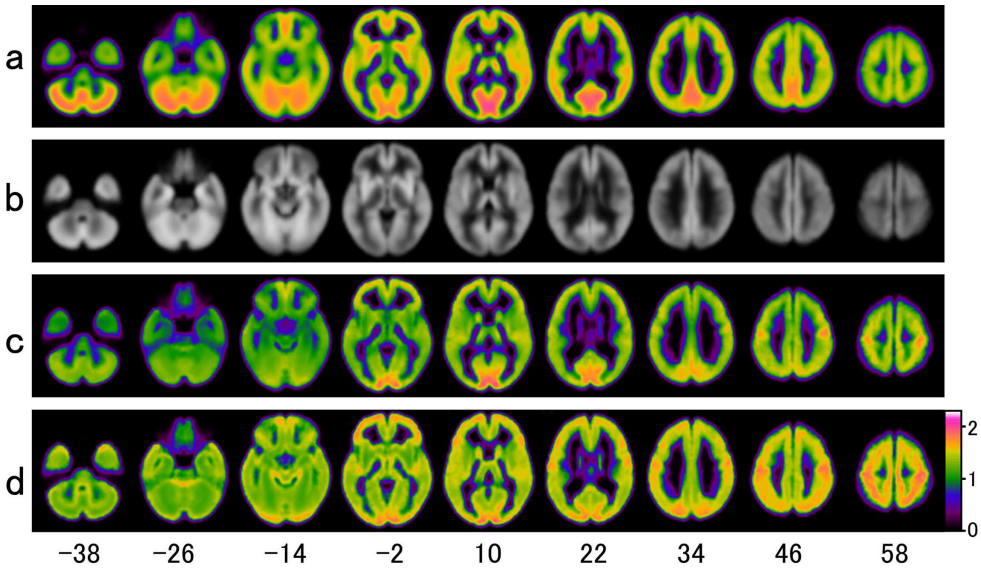

Fig. 1 Mean images of the a) original SPECT, b) GM-MR, c) PVC-SPECT, and d) correction factor. Orientation is in the radiological convention. Values are distances from the AC-PC plane. Range of the correction factor is indicated by a color bar.

Fig. 2 Areas that showed statistically significant decreases in GM concentration with age in the GM images (*left*) and in CBF in the original ^{99m}Tc-ECD SPECT images (*middle*) and in the PVC-SPECT images (*right*) are demonstrated in the standardized glass brain maps.

Fig. 2

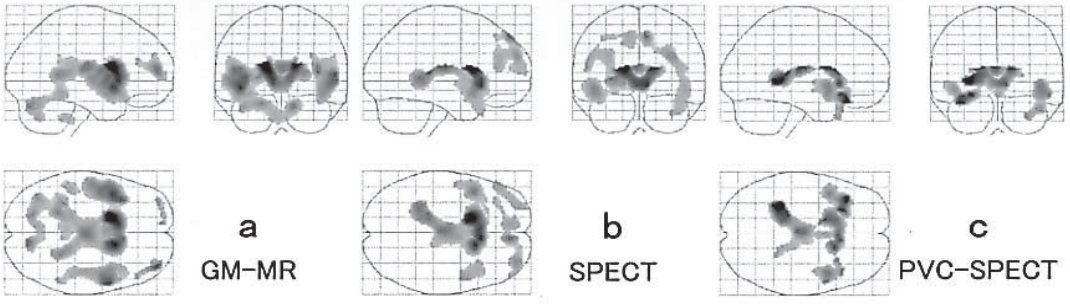

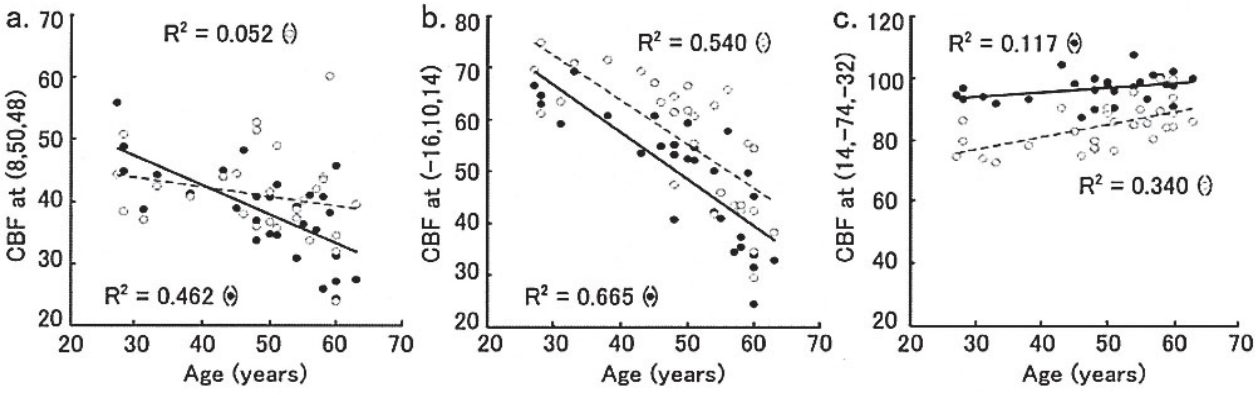

Fig. 3

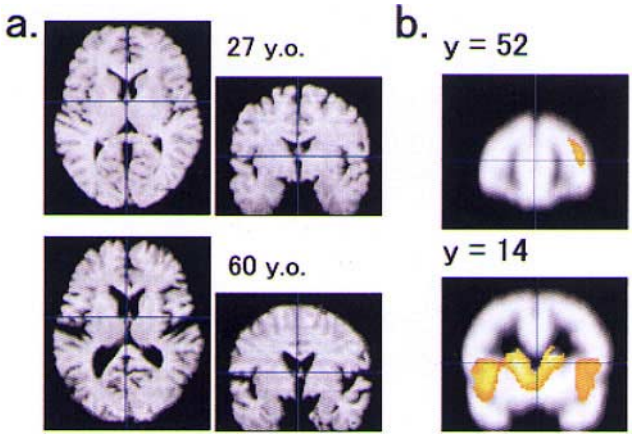

Fig. 4

T1-weighted gradient echo sequence produced a gapless series of thin transverse sections using an SPGR sequence (TE/TR, 7/40 ms; flip angle, 30°; 25-cm field of view; acquisition matrix, 256 × 256; slice thickness, 1.5 mm).

Data processing and analysis

We used Matlab 5.3 (Mathworks, Natick, MA, USA) and SPM99 (http://www.fil.ion.ucl.ac.uk/spm) for MR and SPECT image processing and statistical analysis. PVC of SPECT data was performed as follows, based on the methods developed for PVC for PET,[15,16] applied for SPECT recently.[31]

First, each whole-brain MR image was segmented into a GM, white matter (WM) and cerebrospinal fluid (CSF) space MR image. A binary brain mask for the whole-brain obtained from GM and WM MR images was applied to the corresponding whole-brain MR image to exclude the outer scalp to improve the coregistration of the MR image to the SPECT image. Each of the whole and segmented MR images and the brain mask image were coregistered to the corresponding SPECT images and resliced to adjust the voxel size.[33] These resliced GM and WM images were then convoluted with a 7 mm FWHM isotropic Gaussian kernel, approximating the point spread function of the SPECT device. Regions of interest (ROIs) were automatically extracted from WM-MR images as areas more than 95% in WM concentration using MRIcro software[34] and then overlaid on SPECT images. The multiplication of the WM-MR image by the mean SPECT count for these WM-ROIs yielded a WM-SPECT image. A GM-SPECT image was obtained by subtracting the WM-SPECT image from the SPECT image with an assumption that tracer retention in the CSF space was negligible. A GM mask image that consisted of voxels whose GM concentration was higher than an empirically determined value of 0.25 in the GM-MR image was applied to the GM-MR and GM-SPECT images to exclude activities outside of the brain and around the edge of the GM to avoid a large correction error. Finally, the GM-SPECT image was divided by the GM-MR image, yielding a PVC-SPECT image.

The GM mask image was also applied to the original SPECT image to compare it with the PVC-SPECT image in the same image volume. All GM-MR images, and SPECT and PVC-SPECT images were then spatially normalized to the ICBM 152 template (Montreal Neurological Institute), using linear and nonlinear parameters created from the spatial normalization of the original whole-brain MR images[35,36] and resliced with a final voxel size of 2 × 2 × 2 mm. These normalized images were smoothed with a 12 mm FWHM isotropic Gaussian kernel to compensate for individual differences in the gyral anatomy. We also created a correction factor image by dividing the PVC-SPECT image by the SPECT image. For the analysis of age and gender effects on the GM-MR, SPECT and PVC-SPECT images, the same design of SPM99 (single subject, conditions and covariates) was used. Genders were treated as conditions (female and male) and age as a covariate for each datum. The confounding effect of the global counts of the original SPECT and PVC-SPECT images was removed by proportional scaling to an arbitral global value of 50. The covariates were centered around mean values for each datum. The effects of age and gender were contrasted and thresholded at $t > 3.2$ for SPECT data before and after PVC, corresponding to $p < 0.05$, corrected for multiple comparisons on the basis of a false discovery rate (FDR) procedure.[37–39] For the GM-MR images, the height threshold $t > 4.4$, corresponding to $p < 0.01$, corrected for multiple comparisons by FDR procedure, was used because a large number of voxels survived, which could be a false positive, at $t > 2.6$, corresponding to $p < 0.05$, corrected for multiple comparisons by the FDR procedure.

RESULTS

The mean images of the spatially normalized GM-MR, SPECT, PVC-SPECT, and correction factor images for all subjects are shown in Figure 1. In the mean PVC-SPECT image, GM counts are more homogeneous than in the mean SPECT image, except for the relatively high activity in the medial occipital cortex and pericentral area. The correction factor was inhomogeneous throughout the brain, and it was high in the anterolateral part of the frontal cortex, the posterosuperior part of the parietal cortex and the posterior part of the occipital cortex, whereas it was low in the temporal cortex, the inferomedial part of the occipital cortex and the cerebellum.

In the GM-MR images, statistically significant decreases in GM concentration with age in males were found in the anterolateral prefrontal cortex (PFC), in an area along the lateral sulcus including the inferolateral frontal cortex and anterior temporal cortex, as well as in large areas around the lateral and the third ventricles including the caudate head, thalamus and retrosplenial cortex, bilaterally (Fig. 2a). In females, no statistically significant decrease in GM concentration with age was detected. In the SPECT images, decreases in CBF with age were found only in males, and followed a similar pattern to that found for age effect on GM concentration, in areas of the anterolateral PFC, in an area along the lateral sulcus and large areas around the lateral and the third ventricles, bilaterally (Fig. 2b). In the PVC-SPECT images, we still found decreases in CBF with age in areas along the lateral ventricle and the lateral sulcus, but we did not note any statistically significant decrease with age in the bilateral anterolateral PFCs (Fig. 2c). Figure 3 represents the effects of PVC on CBF in males, in an area in the right anterolateral PFC where the decrease in CBF with age lost its statistical significance after PVC, in an area located around the left caudate head where the decrease in CBF with age remained significant after PVC, and in an area in

Table 1 Areas in which statistically significant decreases were detected on the original SPECT, GM-MR and PVC-SPECT images

size	x	y	z	t	Region
SPECT					
660	34	58	28	4.6	R lateral prefrontal
442	−54	38	16	4.2	L lateral prefrontal
712	48	6	−8	4.0	R insula
310	−16	10	14	7.3	L caudate head
102	−44	14	−10	4.9	L lateral sulcus
GM-MR					
317	38	56	12	5.4	R lateral prefrontal
155	−32	58	8	4.2	L lateral prefrontal
273	54	6	6	4.9	R inferior frontal gyrus
236	−48	−34	18	4.2	L superior temporal gyrus
906	−18	8	16	7.6	L caudate head
225	−4	−38	−40	4.0	Pons
PVC-SPECT					
152	42	24	−28	4.5	R superior temporal gyrus
652	44	8	−6	4.9	R insula
906	−36	26	−18	6.0	L inferior frontal gyrus
122	−30	−42	2	7.1	L lateral ventricle
120	14	16	14	5.5	R caudate head

Size: cluster size in voxels, voxel size = 2 × 2 × 2 mm. (x, y, z): Co-ordinates of maximal significant voxel in a region in mm. t: SPM t statistics. Abbreviations; R: right hemisphere, L: left hemisphere, lateral sulcus: area around the lateral sulcus, lateral ventricle: area around the lateral ventricle.

the right cerebellum where no age effect was detected either before or after PVC. The brain shapes of a young subject and an old subject after spatial normalization and the superimposition of areas that showed statistically significant decreases in GM concentration with age on the mean of spatial normalized GM mask images, are shown in Figure 4. The age effects, which did not change significantly either before or after PVC that were detected around the lateral sulcus and ventricle, located on the margin of the mean GM mask image. We found no statistically significant gender-related difference in any of the images that were analyzed. The areas showing age effects in the GM-MR, SPECT and PVC-SPECT images are summarized in Table 1.

DISCUSSION

Our analyses revealed that the decrease in CBF with age found in the PFC using ^{99m}Tc-ECD SPECT, which lost its statistical significance after PVC, resulted from regional changes in GM concentration with age. We also found regional differences in the effect of PVC on age effects on CBF among areas, that is, CBF decreases with age remained statistically significant in areas around the lateral sulcus and lateral and third ventricles.

Our finding of apparent CBF decreases with age in the anterolateral PFC, in areas around the lateral sulcus and periventricular areas was consistent with previous reports using SPECT and ^{99m}Tc-labeled tracers.[1,2,4–9,12] Our findings were also in line with previous reports on decreases in GM concentration with normal aging,[22,23,25,40] and on the similarity of the pattern of decreases in the brain between CBF and GM.[25] In the present study, we found more areas that showed statistically significant age effects on GM concentration and CBF in males than in our previous report.[26] The difference from the previous report may have been due to the fact that we included young male subjects in the present analysis, although there were differences in image processing and statistical analysis as well.

Several studies have assessed the effect of PVC in normal subjects and conducted comparisons between patients and normal controls. Muller-Gartner et al. described a PVC method for PET images using MRI images, on which we based our present study. They demonstrated an application of the method for human PET studies using ^{11}C-carfentanil, and found a regional increase in the tracer uptake that was not evident before PVC.[16] Using the same method, an apparent decrease in CBF with healthy aging measured by $H_2{}^{15}O$ and PET was considered to have resulted from regional cerebral volume differences among the subjects, which were cancelled by PVC.[30] In the present results, CBF decrease with age in the anterolateral PFC bilaterally detected before PVC was recovered after PVC. The lateral PFC is an area where the largest age effects on GM in healthy old subjects have been reported,[22,41] and our present finding was consistent with a previous study that applied the method for PVC.[30] Our present findings suggest that an apparent CBF decrease in the lateral PFC in healthy old subjects is attributable to PVE due to morphological changes of the brain with age, and that CBF in GM may be preserved in normal aging. The present findings, in agreement with previous studies, demonstrated that PVC can differentiate physiological changes from apparent age effects resulting from brain atrophy with age.

Recently, the method for PVC has also been applied to CBF SPECT using ^{99m}Tc-ECD.[31] The authors have shown that the decreases in CBF with age detected before PVC, in areas around the lateral sulcus and the anterior cingulate gyrus, remained after PVC. Their findings of decrease in CBF with age before and after PVC, around the lateral sulcus bilaterally, were similar to our present results, although there were inconsistencies, which could be due to differences in the SPECT instruments used and the subjects' age range, and we also found these findings along the lateral and third ventricles. The findings can be considered to reflect the true decline in regional CBF with age in these regions, but there could be another reason for these findings. The present study and a few other recent studies[27,31,42] have adopted voxel-by-voxel analysis in a standardized stereotactic space with spatial normalization

techniques, particularly using SPM software, in assessing age effects or in comparisons between patients and controls to avoid subjective ROI placement. Nonlinear spatial normalization techniques employed in SPM, however, attempt to accommodate global brain shape differences, but not to match every structure in the brain exactly.[36] Figure 4a shows the shapes of the spatially normalized brains of a young subject and an old subject, as representative cases. The outer contours of the brains fairly match each other, but the boundary between GM and the ventricles and the lateral sulcus shows obvious discordance between the young and old subjects. The shape of the deep GM, especially the caudate head, was also thin in the old subject. In Figure 4b, areas where age effects were detected in the GM-MR images were superimposed on the mean GM mask image, representing the accordance of the extent to which the presence of GM for each subject was presumed. Areas in the anterolateral PFC were located within the mean GM mask image. Areas around the ventricles and lateral sulcus were, on the other hand, on the edge of the mean GM mask image, which suggests that the detected age effect represented discordance of presumed GM extent depending on age. With the present method, PVC was performed on voxels within the presumed GM extent for each subject. Due to limitations in methods for spatial normalization, it is not possible to match the presumed GM extent among subjects in the standard stereotactic space, resulting in the demonstration of a statistically significant correlation with age, or with other parameters highly correlated with brain atrophy. Although the discordance reflects brain atrophy and, is therefore highly correlated with the age effect itself, it seemed undesirable for the assessment of PVC for age effects in CBF in the present study. The present finding of age effects that could not be changed by PVC was considered to reflect the age-dependent discordance of GM extent resulting from the limitations of available methods for spatial normalization of brain anatomy, and could not be considered to reflect the true physiological CBF changes.

We could not find statistically significant age effects in females in the GM-MR images, which is inconsistent with our previous study.[26] Several studies have indicated that there is more brain atrophy with aging in males than in females,[43,44] and enlargement with age of the ventricles is greater in males than females,[45,46] although a few studies did not find statistically significant male dominance in the ventricular enlargement.[22,44] In the present study, GM-MR images were resliced to adjust the voxel size to that of the SPECT image. PVE in the GM-MR images, therefore, should be larger than those in recent morphometric studies using MRI, and was considered to have resulted in the negative findings with respect to age effect in females, combined with less atrophy in females than in males.

In conclusion, the present results suggest that the regional variability of tracer retention results from regional differences in GM concentration in the brain. The apparent age effects on CBF found in the lateral PFC reflect PVE that is augmented by cortical atrophy with normal aging. On the other hand, because present spatial normalization methods leave morphological mismatches in spatially normalized brain shapes, there could be areas where the effects of PVC on apparent age effects may not be properly assessed using voxel-by-voxel analysis with spatial normalization to the stereotactic space, and can cause difficulty in the interpretation of findings with respect to the presence of physiological changes.

ACKNOWLEDGMENTS

This work was partially supported by the Ministry of Education, Science, Sports and Culture, Grant-in-Aid for Young Scientists (B), 14770439, and by research grants from "R&D promotion scheme for regional proposals" promoted by the Telecommunication Advancement Foundation and the Foundation for Prevention of Dementia.

REFERENCES

1. Goto R, Kawashima R, Ito H, Koyama M, Sato K, Ono S, et al. A comparison of Tc-99m HMPAO brain SPECT images of young and aged normal individuals. *Ann Nucl Med* 1998; 12: 333–339.
2. Waldemar G, Hasselbalch SG, Andersen AR, Delecluse F, Petersen P, Johnsen A, et al. ^{99m}Tc-*d,l*-HMPAO and SPECT of the brain in normal aging. *J Cereb Blood Flow Metab* 1991; 11: 508–521.
3. Markus H, Ring H, Kouris K, Costa D. Alterations in regional cerebral blood flow, with increased temporal interhemispheric asymmetries, in the normal elderly: an HMPAO SPECT study. *Nucl Med Commun* 1993; 14: 628–633.
4. Van Laere K, Versijpt J, Audenaert K, Koole M, Goethals I, Achten E, et al. ^{99m}Tc-ECD brain perfusion SPET: variability, asymmetry and effects of age and gender in healthy adults. *Eur J Nucl Med* 2001; 28: 873–887.
5. Catafau AM, Lomena FJ, Pavia J, Parellada E, Bernardo M, Setoain J, et al. Regional cerebral blood flow pattern in normal young and aged volunteers: a ^{99m}Tc-HMPAO SPET study. *Eur J Nucl Med* 1996; 23: 1329–1337.
6. Mozley PD, Sadek AM, Alavi A, Gur RC, Muenz LR, Bunow BJ, et al. Effects of aging on the cerebral distribution of technetium-99m hexamethylpropylene amine oxime in healthy humans. *Eur J Nucl Med* 1997; 24: 754–761.
7. Martin AJj, Friston KJ, Colebatch JG, Frackowiak RS. Decreases in regional cerebral blood flow with normal aging. *J Cereb Blood Flow Metab* 1991; **11**: 684–689.
8. Krausz Y, Bonne O, Gorfine M, Karger H, Lerer B, Chisin R. Age-related changes in brain perfusion of normal subjects detected by ^{99m}Tc-HMPAO SPECT. *Neuroradiology* 1998; 40: 428–434.
9. Claus JJ, Breteler MM, Hasan D, Krenning EP, Bots ML, Grobbee DE, et al. Regional cerebral blood flow and cerebrovascular risk factors in the elderly population. *Neurobiol Aging* 1998; 19: 57–64.
10. Gur RC, Gur RE, Obrist WD, Hungerbuhler JP, Younkin D, Rosen AD, et al. Sex and handedness differences in cerebral

blood flow during rest and cognitive activity. *Science* 1982; 217: 659–661.
11. Rodriguez G, Warkentin S, Risberg J, Rosadini G, Sex differences in regional cerebral blood flow. *J Cereb Blood Flow Metab* 1988; 8: 783–789.
12. Pagani M, Salmaso D, Jonsson C, Hatherly R, Jacobsson H, Larsson SA, et al. Regional cerebral blood flow as assessed by principal component analysis and (99m)Tc-HMPAO SPET in healthy subjects at rest: normal distribution and effect of age and gender. *Eur J Nucl Med Mol Imaging* 2002; 29: 67–75.
13. Jones K, Johnson KA, Becker JA, Spiers PA, Albert MS, Holman BL. Use of singular value decomposition to characterize age and gender differences in SPECT cerebral perfusion. *J Nucl Med* 1998; 39: 965–973.
14. Hoffman EJ, Huang SC, Phelps ME. Quantitation in positron emission computed tomography: 1. Effect of object size. *J Comput Assist Tomogr* 1979; 3: 299–308.
15. Meltzer CC, Leal JP, Mayberg HS, Wagner HN Jr, Frost JJ. Correction of PET data for partial volume effects in human cerebral cortex by MR imaging. *J Comput Assist Tomogr* 1990; 14: 561–570.
16. Muller-Gartner HW, Links JM, Prince JL, Bryan RN, Mcveigh E, Leal JP, et al. Measurement of radiotracer concentration in brain gray matter using positron emission tomography: MRI-based correction for partial volume effects. *J Cereb Blood Flow Metab* 1992; 12: 571–583.
17. Strul D, Bendriem B, Robustness of anatomically guided pixel-by-pixel algorithms for partial volume effect correction in positron emission tomography. *J Cereb Blood Flow Metab* 1999; 19: 547–559.
18. Rousset OG, Ma Y, Evans AC. Correction for partial volume effects in PET: principle and validation. *J Nucl Med* 1998; 39: 904–911.
19. Videen TO, Perlmutter JS, Mintun MA, Raichle ME. Regional correction of positron emission tomography data for the effects of cerebral atrophy. *J Cereb Blood Flow Metab* 1988; 8: 662–670.
20. Ashburner J, Friston KJ. Voxel-based morphometry—the methods. *Neuroimage* 2000; 11: 805–821.
21. Goldszal AF, Davatzikos C, Pham DL, Yan MX, Bryan RN, Resnick SM. An image-processing system for qualitative and quantitative volumetric analysis of brain images. *J Comput Assist Tomogr* 1998; 22: 827–837.
22. Resnick SM, Pham DL, Kraut MA, Zonderman AB, Davatzikos C. Longitudinal magnetic resonance imaging studies of older adults: a shrinking brain. *J Neurosci* 2003; 23: 3295–3301.
23. Good CD, Johnsrude IS, Ashburner J, Henson RN, Friston KJ, Frackowiak RSJ. A voxel-based morphometric study of ageing in 465 normal adult human brains. *Neuroimage* 2001; 14: 21–36.
24. Good CD, Johnsrude I, Ashburner J, Henson RN, Friston KJ, Frackowiak RS. Cerebral asymmetry and the effects of sex and handedness on brain structure: a voxel-based morphometric analysis of 465 normal adult human brains. *Neuroimage* 2001; 14: 685–700.
25. Van Laere KJ, Dierckx RA. Brain perfusion SPECT: age- and sex-related effects correlated with voxel-based morphometric findings in healthy adults. *Radiology* 2001; 221: 810–817.
26. Inoue K, Nakagawa M, Goto R, Kinomura S, Sato T, Sato K, et al. Regional differences between (99m)Tc-ECD and (99m)Tc-HMPAO SPET in perfusion changes with age and gender in healthy adults. *Eur J Nucl Med Mol Imaging* 2003; 30: 1489–1497.
27. Ibanez V, Pietrini P, Alexander GE, Furey ML, Teichberg D, Rajapakse JC, et al. Regional glucose metabolic abnormalities are not the result of atrophy in Alzheimer's disease. *Neurology* 1998; 50: 1585–1593.
28. Labbe C, Froment JC, Kennedy A, Ashburner J, Cinotti L. Positron emission tomography metabolic data corrected for cortical atrophy using magnetic resonance imaging. *Alzheimer Dis Assoc Disord* 1996; 10: 141–170.
29. Matsuda H, Kanetaka H, Ohnishi T, Asada T, Imabayashi E, Nakano S, et al. Brain SPET abnormalities in Alzheimer's disease before and after atrophy correction. *Eur J Nucl Med Mol Imaging* 2002; 29: 1502–1505.
30. Meltzer CC, Cantwell MN, Greer PJ, Ben-Eliezer D, Smith G, Frank G, et al. Does cerebral blood flow decline in healthy aging? A PET study with partial-volume correction. *J Nucl Med* 2000; 41: 1842–1848.
31. Matsuda H, Ohnishi T, Asada T, Li ZJ, Kanetaka H, Imabayashi E, et al. Correction for partial-volume effects on brain perfusion SPECT in healthy men. *J Nucl Med* 2003; 44: 1243–1252.
32. Koyama M, Kawashima R, Ito H, Ono S, Sato K, Goto R, et al. SPECT imaging of normal subjects with technetium-99m-HMPAO and technetium-99m-ECD. *J Nucl Med* 1997; 38: 587–592.
33. Ashburner J, Friston KJ. Multimodal image coregistration and partitioning—a unified framework. *Neuroimage* 1997; 6: 209–217.
34. Rorden C, Brett M. Stereotaxic display of brain lesions. *Behav Neurol* 2000; 12: 191–200.
35. Ashburner J, Neelin P, Collins DL, Evans A, Friston KJ. Incorporating prior knowledge into image registration. *Neuroimage* 1997; 6: 344–352.
36. Ashburner J, Friston KJ. Nonlinear spatial normalization using basis functions. *Hum Brain Mapp* 1999; **7**: 254–266.
37. Benjamini Y, Hochberg Y. Controlling the False Discovery Rate: a Practical and Powerful Approach to Multiple Testing. *J Royal Stat Soc B* 1995; 57: 289–300.
38. Yekutieli D, Benjamini Y. Resampling based false discovery controlling multiple test procedures for correlated test statistics. *J Statist Plann Inference* 1999; 82: 171–196.
39. Genovese CR, Lazar NA, Nichols T. Thresholding of statistical maps in functional neuroimaging using the false discovery rate. *Neuroimage* 2002; 15: 870–878.
40. Taki Y, Goto R, Evans A, Zijdenbos A, Neelin P, Lerch J, et al. Voxel-based morphometry of human brain with age and cerebrovascular risk factors. *Neurobiol Aging* 2004; 25: 455–463.
41. Raz N, Gunning FM, Head D, Dupuis JH, Mcquain J, Briggs SD, et al. Selective aging of the human cerebral cortex observed *in vivo*: differential vulnerability of the prefrontal gray matter. *Cereb Cortex* 1997; 7: 268–282.
42. Bencherif B, Stumpf MJ, Links JM, Frost JJ. Application of MRI-Based Partial-Volume Correction to the Analysis of PET Images of micro-Opioid Receptors Using Statistical Parametric Mapping. *J Nucl Med* 2004; 45: 402–408.
43. Xu J, Kobayashi S, Yamaguchi S, Iijima K-I, Okada K,

Yamashita K. Gender Effects on Age-Related Changes in Brain Structure. *AJNR Am J Neuroradiol* 2000; 21: 112–118.
44. Gur RC, Mozley PD, Resnick SM, Gottlieb GL, Kohn M, Zimmerman R, et al. Gender differences in age effect on brain atrophy measured by magnetic resonance imaging. *Proc Natl Acad Sci USA* 1991; 88: 2845–2849.
45. Longstreth WT Jr, Arnold AM, Manolio TA, Burke GL, Bryan N, Jungreis CA, et al. Clinical correlates of ventricular and sulcal size on cranial magnetic resonance imaging of 3,301 elderly people. The Cardiovascular Health Study. Collaborative Research Group. *Neuroepidemiology* 2000; 19: 30–42.
46. Davatzikos C, Resnick SM. Degenerative age changes in white matter connectivity visualized *in vivo* using magnetic resonance imaging. *Cereb Cortex* 2002; 12: 767–771.